SYNTHESIS AND CHARACTERIZATION OF FUNCTIONALIZED MESOPOROUS SILICA MCM-41 AS ADSORBENT FOR COPPER IONS REMOVAL

by

Muhammad Hanif Bin Yusoff
15126

Dissertation submitted in partial fulfillment of
the requirement for the
Bachelor of Engineering (Hons)
(Chemical)

May 2014

Universiti Teknologi PETRONAS
Bandar Seri Iskandar
31750 Tronoh
Perak Darul Ridzuan

CERTIFICATION OF APPROVAL

SYNTHESIS AND CHARACTERIZATION OF FUNCTIONALIZED MESOPOROUS SILICA MCM-41 AS ADSORBENT FOR COPPER IONS REMOVAL

by

Muhammad Hanif Bin Yusoff
15126

A project dissertation submitted to the
Chemical Engineering Programme
Universiti Teknologi PETRONAS
in partial fulfillment of the requirement for the
BACHELOR OF ENGINEERING (Hons)
(CHEMICAL)

Approved by,

_____

(Dr Yeong Yin Fong)

UNIVERSITI TEKNOLOGI PETRONAS
TRONOH, PERAK
May 2014

CERTIFICATION OF ORIGINALITY

This is to certify that I am responsible for the work submitted in this project, that the original work is my own except as specified in the references and acknowledgements, and that the original work contained herein have not been undertaken or done by unspecified sources or persons.

_____

MUHAMMAD HANIF BIN YUSOFF

ABSTRACT

Copper ions are one of heavy metal that high in toxicity and can cause pollutant. Removing copper ions has become a major key mostly in chemical industry as heavy metals can bring many negative impacts to living organisms as well as pollute the environment. Due to that, many researches have been conducted to remove copper ions which include chemical precipitation, reverse osmosis, ion exchange, ultra filtration and adsorption. Adsorption is the most preferential technology mainly attributed to its ease of availability and economic efficiency. Study showed that amino functionalized mesoporous silica, MCM-41 has great potential in copper ions adsorption as it has high selectivity of heavy metal separation. Therefore, this research work is focuses on the synthesis of functionalized MCM-41 tertiary amino group via co-condensation method and the performance of the synthesized adsorbent on copper ion removal. The resulting adsorbent will be characterized using different analytical tools such as Fourier Transform Infrared (FTIR) and Brunauer-Emmett-Teller (BET). The adsorbent then was tested for removal of copper ions. Based on that, the results were analyzed by adsorption isotherm and kinetics model for adsorption study for the adsorbent on copper ion. The adsorption process on modified MCM 41 was well described by the Langmuir Model and Pseudo-Second-Order model. For percentage of copper ions removal,10% AEPTMS – MCM 41 have the highest percentage removal that is 57.4%.. In summary, 10% AEPTMS – MCM 41 was an excellent adsorbent in the field of copper ions removal.

ACKNOWLEDGEMENT

First and foremost, I would like to thank ALLAH S.W.T. for giving me the strength and good health throughout my Final Year Project.

I would like to express my gratitude to my supervisor, Dr Yeong Yin Fong for giving me the opportunity to work under her for my Final Year Project. Her valuable guidance, constructive criticism and support would not be forgotten.

Besides that, I would like to seize this opportunity to thank to all parties who has contributed along the process in accomplishing my Final Year Project. Special appreciation to all staffs and technicians from Chemical Department for their full support, encouragement and guidance.

Last but not least, the appreciation goes to my family and my friends who had been supporting me, sharing ideas and given me encouragement and strength during the entire period of this project.

TABLE OF CONTENTS

List of Figures

List of Tables

CHAPTER 1
INTRODUCTION

1.1 Background of Study

Industrial heavy metal pollution has become a serious environmental and sanitary problem all over the world in recent years. Heavy metals not only have toxic and harmful effects on organisms living in water, but also accumulate throughout the food chain and may also affect human beings (Heidari, Younesi, & Mehraban, 2009). Heavy metals give negative impact to living organism, especially on human being. Although living organisms need certain amount of "heavy metal" for living, excessive amount can bring damage to the organism. Other than that, these toxic elements in soils are non-biodegradable and, therefore, are extremely persistent in the environment (Zhou et al., 2014). Because of that, many research, study and method were created in order to separate and remove heavy metal ions.

Since heavy metals have toxic effects on the environment and human life, the removal of heavy metal ions from polluted waters is currently one of the important topics for environmental challenges. Different processes are used in industry to remove these metals from aqueous media, such as ion exchange, adsorption, reverse osmosis, chemical precipitation being, sedimentation, filtration, electrodialysis, etc(Pérez-Quintanilla, Sánchez, del Hierro, Fajardo, & Sierra, 2007). But with the addition in pollution involving heavy metal, there is an increase in demand to produce an adsorbents of higher efficiency for removal of heavy metal ions than those available adsorbents (Heidari et al., 2009). One of the potential absorbent for removal of heavy metal ions is mesoporous silica, MCM-41.

Mesoporous silica, MCM-41 by cooperative assembly of silica and surfactants, has attracted a great deal of research interest in recent years. These

mesoporous materials have a large pore size (1.5–10 nm) and a high internal surface area (up to 1200 m^2/g). Therefore, it can be used as catalyst, adsorbent, absorbent and etc.

Due to its potential application in adsorption of heavy metal ions, MCM-41 has attracted much interest among the researchers. The surface of mesoporous silica materials can be readily functionalized with organic groups in order to change their characteristics and achieve specific purposes (Lee et al., 2011). For synthesizing of this adsorbent, modification of mesoporous silica MCM-41 can be carried out by post-synthesis grafting and co-condensation methods. In general, post-synthesis grafting method can be done by grafting the surface of the preformed silica by means of silanol groups reactions with an organoalkoxysilane compound supporting the active functional group (Taib, Endud, & Katun, 2011), whereas co-condensation method used sodium hydroxide catalyzed reactions on tetraethoxysilane (TEOS) with various organoalkoxysilanes in the presence of a low concentration of cetyltrimethylammonium bromide (CTAB) surfactant (Huh., Wienc., Yoo., Prusk., & Lin., 2003). In the present work, removal of heavy metal ios; copper ion by using functionalized mesoporous silica MCM-41 adsorbent synthesized by co-condensations method will be focused.

1.2 Problem Statement

Heavy metal ions were harmful and toxic to living organisms. One ways to remove heavy metal ions is by absorption process by mesoporous silica MCM-41 absorbent.

Although mesoporous silica MCM-41 absorbent had been identified as a potential candidate for heavy metal ions removal, it performance in heavy metal ions is yet to be improved. Besides, synthesis of functionalized mesoporous silica MCM-41 using tertiary amine-functional group remains a new task. Therefore, the present work focuses on the development of this new type of adsorbent and its performance in copper ions removal

1.3 Objective

The objectives of the present research are:

i. To synthesis functionalized mesoporous silica MCM-41 adsorbent by using tertiary amine-functional group (3-[2-(2-aminoethylamino) ethylamino]propyltrimethoxysilaneAEPTMS).
ii. To characterize the resultants absorbent using Brunauer-Emmett-Teller (BET) analysis and Fourier transform infrared (FTIR).
iii. To test the performance of the absorbent in removal of copper ions.

1.4 Scope of Study

In order to complete this research, several scope of study has to be completed.

- Synthesize of functionalized mesoporous silica MCM-41 absorbent by tertiary amine-functional group using co-condensation method.
- Characterization study of the resultants absorbent (functionalized mesoporous silica MCM-41) using analytical tools such as Brunauer-Emmett-Teller (BET) and Fourier transform infrared (FTIR).
- Test the absorbent in removal of heavy metal (copper ions) and analyze the performances of the absorbent.

CHAPTER 2
LITERATURE REVIEW

2.1 Effect of heavy metal ions

Heavy metals released into the environment from plating plants, mining, metal finishing, welding and alloy manufacturing pose a significant threat to the environment and public health. The major concern with heavy metals is their ability to accumulate in the environment and cause heavy metal poisoning. Unlike some organic pollutants, heavy metals are not biodegradable and cannot be metabolized or decomposed (Ge, Li, Ye, & Zhao, 2012). Recently, this environmental damage has been monitored by modern technology. However, the environmental pollution still occurs because of problems of management of the liquid phase environment (Wang, Tsai, Lo, & Tsai, 2008).

Heavy metal pollution caused by lead, copper, chromium, cadmium, nickel and arsenic is most serious to the human body. Concentrations of 0.005 mg/l (for Pb^{2+} and Cr^{3+}), 0.001 mg/l (for Cd^{2+}, Ni^{2+}, and As^{5+}) and 0.1 mg/l (for Cu^{2+}), will cause humans to fall ill (Wang et al., 2008). Therefore, removal of heavy metal ions is an important task in the field of water purification.

The amounts of heavy metal ions are present in relatively low concentrations. Although, the trace concentrations of some heavy metals like copper and cadmium is essential, they are toxic in large amount. Accumulation of lead and cadmium can cause cancer and brain damage as well as poisoning (Huang et al., 2012). Silver is known to be a toxic environmental pollutant with hazardous effects in aquatic ecosystems. Mercury is also one of the most hazardous metals affecting the central nervous system (Mashhadizadeh, Amoli-Diva, Shapouri, & Afruzi, 2014).

Acute exposure to Zn(II) causes health problems such as stomach cramps, skin irritations, vomiting, nausea, and anemia. Very high levels of zinc can damage the pancreas, disturb the protein metabolism and cause arteriosclerosis (Pérez-Quintanilla et al., 2007). Other than that, an excess adsorption of Cu causes Wilson's disease, and Cu(II)-ions are deposited in the brain, skin, liver, pancreas and myocardium (Ahalya, Ramachandra, & Kanamadi, 2003). Lead can cause central nervous system damage. Lead can also damage the kidney, liver and reproductive system, basic cellular processes and brain functions (Fu & Wang, 2011). Due to many negative effects on heavy metal ions, it creates many great concerns in health aspect which makes these ions removal becomes a major key in the industry.

Table 1 show types of heavy metals and it effect on human health with their permissible limits. In general, based on table 1, many major sources of heavy metal come from industrial especially chemical industry. Besides, heavy metal can cause negative impact on human health if the amounts taken exceed the permissible level. For copper ions, the sources come from chemical industry, mining, pesticide production and metal piping. It can give damage to liver and kidney if exceed permissible level of 0.1 mg/l.

Table 1: Types of heavy metals and effect on human health (Singh, Gautam, Mishra, & Gupta, 2011).

Pollutant	**Major sources**	**Effect on human health**	**Permissible level(mg/l)**
Arsenic	Pesticides, fungicides, metal smelters	Bronchitis, dermatitis, poisoning	0.02
Cadmium	Welding, electroplating, pesticide fertilizer, Cd and Ni batteries	Renal dysfunction, lung disease, lung cancer, bone defects, increased blood pressure, kidney damage, bone narrow	0.06
Lead	Paint, pesticide, smoking, automobile, mining, burning of coal	Mental retardation in children, development delay, sensor neural deafness, acute or chronic damage	0.1

		to nervous system, liver, kidney, gastrointestinal damage	
Manganese	Welding, fuel addition, ferromanganese production	Inhalation or contact causes damage to central nervous system	0.26
Mercury	Pesticides, batteries, paper industries	Tremors, gingivitis, minor psychological changes, damage to nervous system	0.01
Zinc	Refineries, brass manufacture, metal plating, plumbing	Corrosive effect on skin, damage to nervous membrane	15
Chromium	Mines, mineral sources	Fatigue, damage to nervous system, irritability	0.05
Copper	Mining, pesticide production, chemical industry, metal piping	Anemia, liver and kidney damage, stomach and intestinal irritation	0.1

2.2 Existing method on heavy metal ions removal

Due to concerns on negative effects on heavy metal, research on removal of these ions had been conducted crucially. The commonly used procedures for removing metal ions from aqueous streams include chemical precipitation, reverse osmosis, ion exchange, ultra filtration and adsorption (Ahalya et al., 2003). The details of the process will be discussed in the following section. However, these processes are expensive, not fully effective and generates the secondary effluent such as sludge which created management (Singanan & Peters, 2013).

2.2.1 Chemical precipitation

In precipitation processes, chemicals react with heavy metal ions to form insoluble precipitates. The forming precipitates can be separated from the water by sedimentation or filtration. And the treated water is then decanted and appropriately discharged or reused. The conventional chemical

precipitation processes include hydroxide precipitation and sulfide precipitation (Fu & Wang, 2011). Chemical precipitation pose a significant problem in terms of disposal of the precipitated wastes(Argun & Dursun, 2006)

2.2.2 Reverse osmosis (RO)

Reverse osmosis is the process of forcing a solvent from a region of high solute concentration through a membrane to a region of low solute concentration by applying a pressure in excess of the osmotic pressure. These processes only give good result when dealing with low concentration of heavy metal. With low heavy metal concentration the permeate flux was sharply decreasing whilst with higher heavy metal concentration the decline is linear (Bakalár, Búgel, & Gajdošová, 2009).

2.2.3 Ion Exchange

In this process, metal ions from dilute solutions are exchanged with ions held by electrostatic forces on the exchange resin. The disadvantages include: high cost and partial removal of certain ions (Ahalya et al., 2003),(Argun & Dursun, 2006).

2.2.4 Ultrafiltration

The general idea is that the surfactant produces large amphiphilic aggregate micelles when it is added to aqueous streams at a concentration higher than its critical micelle concentration (CMC). The metal ions and dissolved organic compounds can be mostly trapped by the micelles if they tend to be strongly attracted by the micelle surface and be solubilized in the micelle interior, respectively. The solutes can be retained after trapping with the micelles, whereas the untrapped species readily pass through the ultrafiltration membranes. The advantages of this method are the low-energy requirements involved in the ultrafiltraion process and its high removal

efficiency owing to the effective trapping of solutes by the micelles (Juang, Xu, & Chen, 2003).

2.2.5 Adsorption

This process use adsorbent that had been functionalized to absorb heavy metal ions. it is a renewable resource, and does not need to be regenerated after it has been used to capture the metals (Argun & Dursun, 2006). There were few examples for adsorbent used such as MCM-41; diamine modified MCM-41, activated carbon and zeolite.

From table 2, the most promising adsorbent was mesoporos silica MCM-41 adsorbent synthesize from diamine group. This is because the adsorbent contain large surface area with nano-size pores compares to other adsorbent. The current state-of-the-art methods for synthesize this adsorbent is post-synthesis grafting and co-condensation method (Huh. et al., 2003). Even though the price for MCM 41 adsorbent is relatively high contrast to other adsorbent commonly used for this application, MCM 41 prove to be useful high-capacity adsorbents because the adsorbent can be economically regenerated while maintaining high adsorption capacities for the analyte of interest after multiple use (Idris et al., 2011)

Table 2: Type of adsorbent with adsorbent removal and its disadvantage.

Type of adsorbent	**Adsorbent removal of Cu^{2+} at 25^0C**	**Disadvantage**
Diamine Modified MCM-41	66.577 mg/g (W. Yang et al., 2013)	High cost, expensive (Idris et al., 2011)
Zeolite (SAPO 34)	28.57 mg/g (Ji et al., 2012)	Difficult to separate from solution after adsorption (Ji et al., 2012)
Activated carbon	0.587–0.660 mg/g (Lo, Wang, Tsai, & Lin, 2012)	Largely economic; expensive (Lo et al., 2012)

Table 3 shows the disadvantages of chemical precipitation, reverse osmosis, ion exchange, ultrafiltration and adsorption process in term of heavy metal ions removal. Although heavy metal ions have many removal process, each process have disadvantages and what we can conclude is adsorption process show the most promising technique for heavy metal ions removal.

Table 3: Disadvantages of removal of heavy metal ions procedure

Type of procedure	Disadvantages
Chemical precipitation	problem in terms of disposal of the precipitated wastes (Argun & Dursun, 2006)
Reverse osmosis	only give good result when dealing with low concentration of heavy metal (Bakalár et al., 2009).
Ion exchange	high cost and partial removal of certain ions (Ahalya et al., 2003),(Argun & Dursun, 2006).
Ultrafitration	high energy costs, highly susceptible to fouling and are generally difficult to clean (Juang et al., 2003)
Adsorption	High cost (Idris et al., 2011)

2.3 Characteristics of Functionalized Mesoporous Silica MCM-41

2.3.1 Mesoporous Silica MCM-41

Various studies on the adsorptive application of MCM 41 have been conducted in various environmental applications. The research conducted for MCM 41 by using both unfunctionalized and functionalized silica. In general, mesoporous silica MCM-41 is produced by removing the surfactant using calcination or extraction from the mesostructured silica-micelle composite. The wall of the adsorbent was made up from amorphous silica network (Yokoi, Kubota, & Tatsumi, 2012).

Due to the large surface area of such structures with nano-size pores, mesoporous materials are considered as a good choice for catalytic systems supports for sophisticated materials, etc. Other than that, one interesting property of a mesoporous material, on the other hand, can be its adsorption capacity, which means that a large amount of the material touching its surface may remain attached to the surface until a high-temperature desorption process is applied(Zamani, Illa, Abdollahzadeh-Ghom, Morante, & Rodríguez, 2009).

Figure 1 show the structure for mesoporous silica MCM-41 in scale of 40nm. Mesoporous materials has nanosize pores whose size in the range 2–50 nm in structure has been expected for applications of adsorbent, catalyst carrier, separation membrane, fixing agent for biomolecule and semiconductor cluster, functional electronics and photonics materials (Nagata, Takimura, Yamasaki, & Nakahira, 2006)

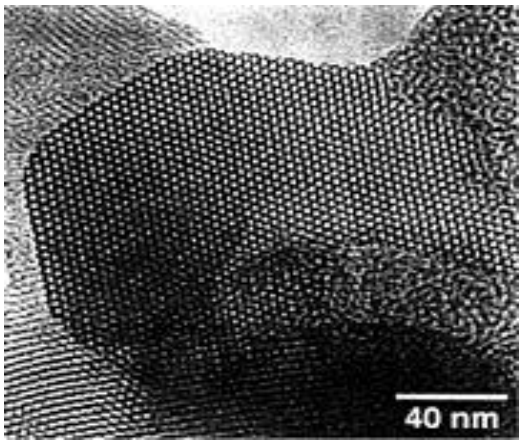

Figure 1: TEM image of mesoporous silica MCM-41 [Nagata et al, 2006]

Besides, MCM-41 is promising as catalysis, adsorption, separation and host-guest compounds. In particular, the uniform, rod-like pore structure of MCM-41 as pure silica materials is ideal host material for semiconductors due to their degree of order and the large band gap of SiO_2, which serve as barrier material (J. Yang, Tao, Ma, & Frost, 2006). MCM-41 combines a myriad of attractive properties including ordered pores systems with tunable pore diameters (in range 2-10 nm),large pore volumes (1cm3/g), pore sizes (1.5-30 nm), high hydrocarbon sorption capacities, high Brunauer-Emmett-Teller, BET surface area (700-1200 m2/g), well-ordered hexagonal structures and high density of surfaces silanol (J. Yang et al., 2006).

2.3.2 Functionalized mesoporous silica MCM-41

For functionalized MCM-41, surface modification of the mesopores can be achieved using direct co-condensation or post-synthesis grafting methods (Yokoi et al., 2012). Surface area of mesoporous silica materials can be readily functionalized with organic group to change their characteristics and purposes (Lee et al., 2011). Functionalized MCM 41has shows positive result in removing heavy metals in aqueous solutions. Generally, the physical and chemical properties for functionalized MCM-41 are slightly the same with pure mesoporous silica MCM-41. However, functionalized MCM-41 has more improvement in both properties due to additional functionalized group such as amine group. Figure 2 show the SEM image for functionalized mesoporous silica MCM-41 in scale of 20 nm and 50 nm.

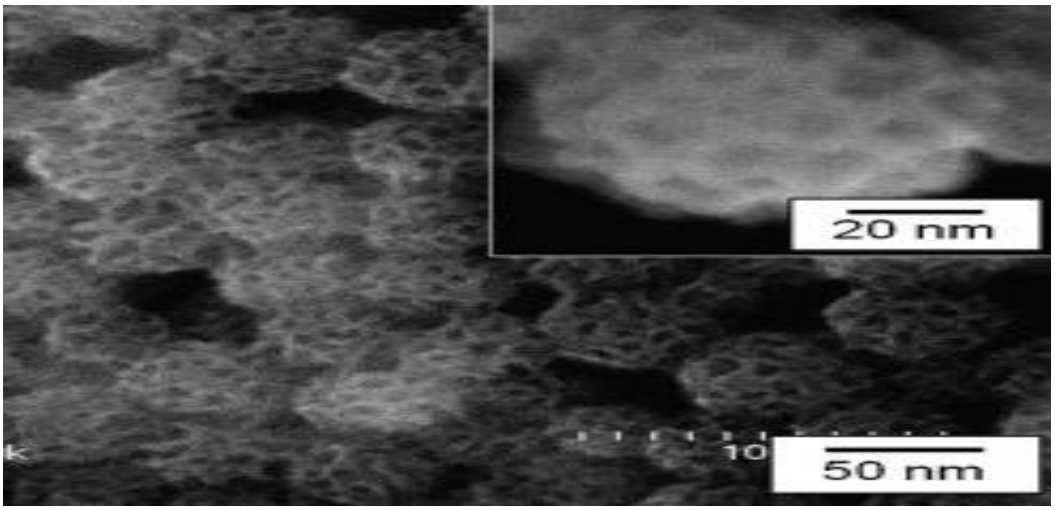

Figure 2: Image of functionalized mesoporous silica nanoparticles (Nandiyanto, Kim, Iskandar, & Okuyama, 2009).

Table 4 shows the adsorbent and its adsorption capacities. From table 4, diamine demonstrated the highest adsorption capacity follows by other functionalized adsorbent. For copper ions adsorption, the maximum adsorption capacity of functionalized amino-mesoporous (66.67 mg/g) is much higher compare to pure. The more amino groups in the mesoporous materials, the more copper ions the materials can adsorb (Yuan et al., 2013).

Table 4: Mesoporous adsorbent and its adsorption capacities for Cu(II) at **25 ^{0}C (W. Yang et al., 2013)**

Mesoporous adsorbents	**Adsorption capacities for Cu(II) at 25 ^{0}C (mg/g)**
Diamine MCM-41	66.67
Modified SA-SBA-15 mesoporous silica	59
Aminopropyl-MCM-41	30.5
Functionalized mesostructured silica containing magnetite	31.8
Mercaptopropyl-functionalized porous silica	13

Compare to pure MCM-41, functionalized MCM-41 has a large surface area with a large number of surface silanol groups, higher average pore size and higher pore size distribution than commonly prepared MCM-41(Idris et al., 2011). Besides, amine groups are reported to improve the adsorption efficiency of heavy metal ions when added to the surface of mesoporous silica MCM-41 (Lee et al., 2011).

Other than that, the pore size of MMC 41is large enough to provide a mixture of large molecules. The high density of silanol groups on the pore wall is valuable to the functional groups with a large coverage (Yokoi et al., 2012). In fact, a lot of surface modifications have been conducted to improve and create new functions for the surfaces. Thus, provide them with a wide range of applications in catalysis, adsorption, separation, chromatography, *etc.,* for bulky molecules that can't enter micro pores of zeolites (Yokoi et al., 2012). So, based on various mesoporous materials studied, it showed that mesoporous silica has found a great interest due to its promising physical and chemical properties (Zamani et al., 2009).

2.4 Synthesis MCM-41 using co-condensation method

Co-condensation method of mesoporous silica MCM-41 is based on sodium hydroxide catalyzed reactions on tetraethoxysilane (TEOS) with various organoalkoxysilanes in the presence of a low concentration of cetyltrimethylammonium bromide (CTAB) surfactant (Huh. et al., 2003). This method differ from post-synthesis grafting method that based on the silylation of organoalkoxysilane with surface silanol groups on the mesopores of the pre-fabricated mesoporous silica (Yokoi et al., 2012), that utilizes silanol group of mesoporous silicates as anchoring sites to graft organic functional groups, metal complexes and metal oxide centers (Teraoka et al., 2001).

For co-condensation method, the organoalkoxysilanes used can be vary such as 3-aminopropyltrimethoxysilane (APTMS), N-(2-aminoethyl)-3-aminopropyltrimethoxysilane (AAPTMS), 3-[2-(2-aminoethylamino)ethylamino]propyltrimethoxysilane (AEPTMS), ureidopropyltrimethoxysilane (UDPTMS), 3-isocyanatopropyltriethoxysilane

(ICPTES), 3-cyanopropyltriethoxysilane (CPTES), and allyltrimethoxysilane (ALTMS) (Huh. et al., 2003). In this project, the synthesize of functionalized mesoporous silica MCM-41 will using AEPTMS as the organoalkoxysilanes.

Figure 3 shows the general process flow of synthesis of tertiary amine functionalized mesoporous silica MCM-41. The organoalkoxysilanes used for process in Figure 3is 3-[2-(2-aminoethylamino)ethylamino]propyltrimethoxysilane (AEPTMS).

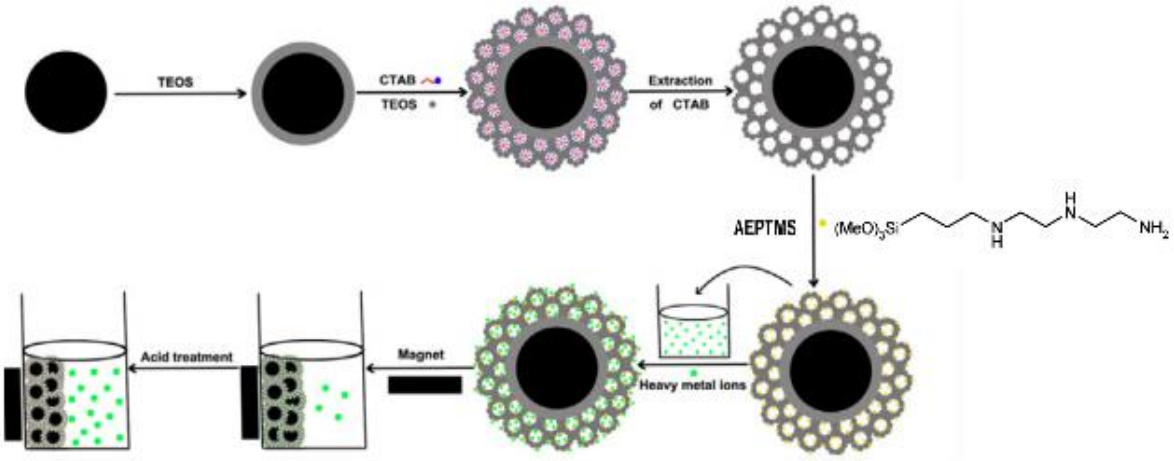

Figure 3: Process flow of synthesize of mesoporous silica MCM-41

The main advantages of of co-condensation method over post-grafting is the resulting homogeneous distribution of organic groups over the MHTF pore and wall surfaces. The acid-base behaviour of amine group in MHTF obtain by co-condensation method depends on the nature of the metal oxide matrix. Fraction of amine functionalities available for reaction depends strongly on the synthesis route; ~16% of them available in co-condensed films (Calvo, Joselevich, Soler-Illia, & Williams, 2009)

As conclusion, in the present project, tri-amine functionalized MCM-41 will be synthesized and characterized. It performance on the removal of copper ions will be tested. Theoretically, by comparing to diamine MCM-41, tri amine MCM -41 is expected to enhance the removal efficiency of copper ions.

CHAPTER 3
METHODOLOGY AND PROJECT ACTIVITY

In the present project, tertiary amine functionalized MCM-41 will be developed by using co-condensation method.

3.1 Project flow chart

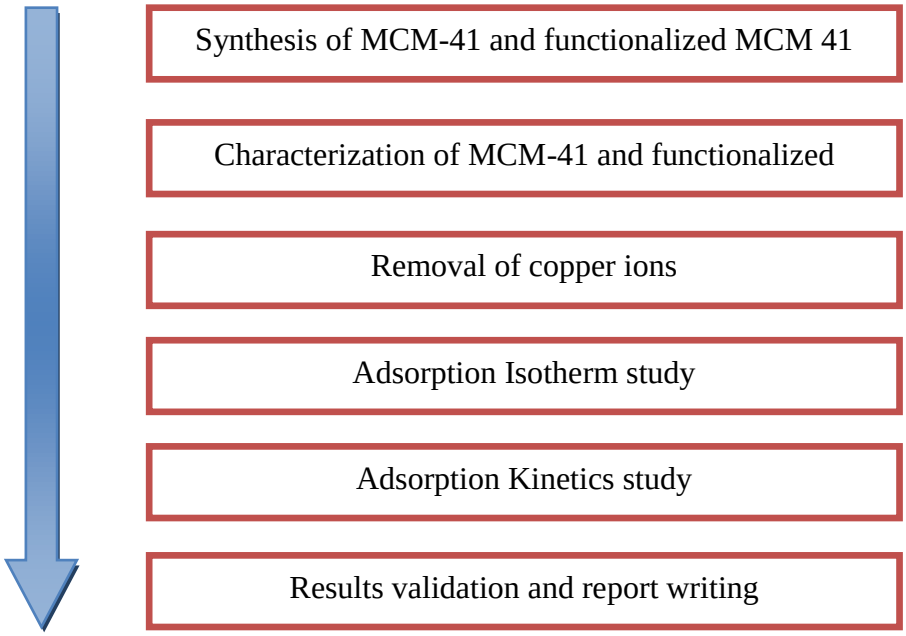

Figure 4: Project Flow Chart

Figure 4 shows process flow chart of this project. Synthesis of MCM-41 and functionalized adsorbent will be conducted by using co-condensation method. After that, characterization study will be conducted to identify the absorbent characteristic using analytical tools such as BET and FTIR. Later, experiments will be conducted to test the performance of MCM-41 and functionalized MCM 41 on removal of copper ions. The results from the experiment will be used for adsorption isothermal and kinetics analysis.

3.2 Experimental procedure for sample synthesize

The method for the synthesis of pure MCM-41 and functionalized AEPTMS MCM-41 are as follows (Huh. et al., 2003):

3.2.1 Synthesize of pure MCM-41:

1. Mixture of CTAB (2.0 g, 5.49 mmol), 2.0 M of NaOH(aq) (7.0 mL, 14.0 mmol), and H2O (480 g, 26.67 mol) was heated at 80 °C for 30 min to reach pH 12.3.
2. To this clear solution, TEOS (10.53 g, 50.55 mmol) were added sequentially and rapidly via injection.
3. A white precipitation was observed after 3 min of stirring at ca. 550 rpm.
4. Temperature of the mixture was maintained at 80 °C for 2 hour.
5. The products were isolated by a hot filtration, washed with copious amount of water and methanol, and dried under vacuum.
6. An acid extraction was performed in a methanol (100 mL) mixture of concentrated hydrochloric acid (1.0 mL) and as-made materials (1.0 g) at 60 °C for 6 h.
7. Resulting surfactant-removed solid products were filtered and washed with water and methanol, and then dried under vacuum.
8. Solid products were label as MCM-41.

3.2.2 Synthesize of functionalized AEPTMS MCM-41:

1. For synthesis of 10% AEPTMS MCM-41, the method described in section 3.2.1 is followed by adding different composition of AEPTMS. For example, for synthesis of 10% AEPTMS MCM 41, TEOS (9.34 g, 44.8 mmol) and APTMS (1.03 g, 5.75 mmol) were added sequentially and rapidly via injection. Label the sample as 10% AEPTMS MCM-41.

2. For synthesis of 20% AEPTMS MCM-41, the method described in section 3.2.1 is followed by adding different composition of AEPTMS. For example, for synthesis of 10% AEPTMS MCM 41, TEOS (8.425 g, 40.44 mmol) and APTMS (2.683 g, 10.11 mmol) were added sequentially and rapidly via injection. Label the sample as 20% AEPTMS MCM-41.

3.3 Characterization study of sample

Table 5 shows the analytical tools of BET and FTIR with general description.

Table 5: Type of analytical tools

Analytical tools	Description
Brunauer-Emmett-Teller, BET	To measure the pore characteristics and surface area of the sample
Fourier transform infrared (FTIR)	To verify the functional group of tertiary amine functionalized MCM-41

3.4 Adsorption Cu^{2+} removal study.

3.4.1 Procedure for Adsorption Kinetics Study

1. 50 mg of sample from synthesis of mesoporous silica MCM-41 was stirred in 50 mL of a copper nitrate solution for 24 hours at room temperature. The initial concentration of copper nitrate was 10 mg/L.
2. The sample was taken every 7, 15 and 24 hours and the concentration of copper nitrate was measured by atomic absorption spectroscopy (AAS).
3. Graph of concentration for atomic absorption spectroscopy versus time was plotted.

4. For standard calibration curve, copper nitrate solution of 2 mg/l, 4 mg/l, 6 mg/l and 8 mg/l was prepared and the metal concentration of the solution was determined by atomic absorption spectroscopy (AAS).

3.4.2 Procedure for Adsorption Isotherms Study

1. 50 mg of sample from synthesis of mesoporous silica MCM-41 was stirred in 50 mL of a copper nitrate solution for 24 hours at room temperature. The concentration of copper nitrate was 2.5, 5.0, 7.5 and 10 mg/L.
2. The sample was taken after 24 hours and the concentration of copper nitrate was measured by atomic absorption spectroscopy (AAS).
3. Graph of concentration for atomic absorption spectroscopy versus concentration of copper nitrate was plotted.
4. For standard calibration curve, copper nitrate solution of 2 mg/l, 4 mg/l, 6 mg/l and 8 mg/l was prepared and the metal concentration of the solution was determined by atomic absorption spectroscopy.

The equilibrium adsorption capacity for adsorbent (Yuan et al., 2013):

$$R\% = [(C_i - C_e) \times C_i] * 100 \quad (1)$$

where,

C_0 and C_e= initial and equilibrium concentrations of the adsorbents (mg/L),

3.5 Adsorption isothermal model

In this project, two isotherm models will be tested.

The saturated adsorption capacity represented by using Langmuir model as shown as follows (Yuan et al., 2013):

$$q_e = (KL * C_e) / (1 + [a_L * C_e]) \quad (2)$$

The Freundlich equation can be applied to non ideal sorption on heterogeneous surfaces or multi-layer sorption and is expressed as follows (Yuan et al., 2013):

$$q_e = (K_f * C_e^{nF}) \quad (3)$$

where,

q_e = Adsorbate concentration in equilibrium (mg/g).

C_e = Adsorbate concentration for aqueous phase at equilibrium (mg/L).

K_L (L/g) and a_L (L/mg) = Langmuir isotherm parameters.

K_F (L/g) = Freundlich parameter.

n_F = heterogeneity factor.

3.6 Adsorption kinetics models

The initial copper ion concentration was selected as 10 mg/L. The adsorption capability of adsorbent for time t, qt (mg/g), was calculated by using equation (4) as follows(Yuan et al., 2013):

$$q_t = [(C_0 - C_t) \times V] / M \quad (4)$$

where,

$C_0$and C_t (mg/L) = initial adsorbates concentration for time t.

M = mass for adsorbent (g).

V = volume of adsorbate (L).

Two kinetic models: the pseudo-first-order and pseudo-second-order equations will be used.

Pseudo-first-order kinetic model is shown as follows(Yuan et al., 2013):

$$\ln(q_e - q_t) = \ln q_e - k_1 t \quad (5)$$

Pseudo-second-order kinetic model is shown in Equation (6) as follows(Yuan et al., 2013):

$$t / q_t = (1 / k_2 q_e^2) + t / q_e \quad (6)$$

where,

q_e and q_t = adsorbed amounts of metal ions at equilibrium and at time t, respectively, mg/g,

k_1= rate constant of pseudo-first-order adsorption, min−1

k_2 = rate constant of second-order adsorption, g mg−1 min−1

t = time

3.7 The chemicals and apparatus.

3.7.1 Chemicals:

- Cetyltrimethylammonium bromide (CTAB)
- Sodium hydroxide
- Water
- TEOS
- APTMS
- Methanol
- Concentrated hydrochloric acid
- Copper (Cu^{2+})

3.7.2 Apparatus

- Beaker
- Conical flask
- Filter paper
- Filter funnel
- Electronic heater and stirring plate
- Retort stand
- Stopwatch
- Test tube
- Magnet

3.8 Key milestones

3.8.1 Table 6 shows key milestones of current project for FYP 1

Table 6: Key milestones for FYP 1

Milestone	Date
Submission of Extended Proposal Defense	Week 7
Proposal Defense Presentation	Week 8
Submission of Interim Draft Report	Week 13
Submission of Interim Final Report	Week 14

3.8.2 Table 7 shows key milestones of current project for FYP 2

Table 7: Key milestones for FYP 2

Milestone	Date
Submission of Progress Report	Week 8
Pre SEDEX	Week 10
Submission of Draft Final Report	Week 11
Submission of Dissertation (Soft Bound)	Week 12
Submission of Technical Paper	Week 12
Viva	Week 13
Submission of Project Dissertation (Hard Bound)	Week 15

3.9 Gantt Chart

Table 8 shows the Gantt chart of the current project for FYP I

Table 8: Gantt Chart for FYP 1

NO	DETAIL / WEEK	1	2	3	4	5	6	7	8	9	10	11	12	13	14
1	Selection of Project Topic														
	Problem statement and analysis of project														
2	Preliminary Research Work and Preparing Proposal														
3	Submission of Extended Proposal Defence														
4	Preparation for Oral Proposal Defence														
	Oral Proposal Defence Presentation														
7	Project work continues														
	Preparation of Interim Report														
8	Submission of Interim Draft Report														
9	Submission of Interim Final Report														

Process

Suggested Key Milestones

Table 9 shows the Gantt chart of the current project for FYP 2

Table 9: Gantt Chart for FYP 2

NO	DETAIL / WEEK	1	2	3	4	5	6	7	8	9	10	11	12	13	14	15
1	Project Work Continues															
2	Submission of Progress Report															
3	Project Work Continues															
4	Pre-SEDEX															
5	Submission of Draft Final Report															
6	Submission of Dissertation (soft bound)															
7	Submission of Technical Paper															
8	Viva															
9	Submission of Project Dissertation (Hard Bound)															

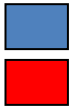

CHAPTER 4
RESULTS AND DISCUSSION

4.1 Characterization Study of Samples

4.1.1 FTIR Analysis

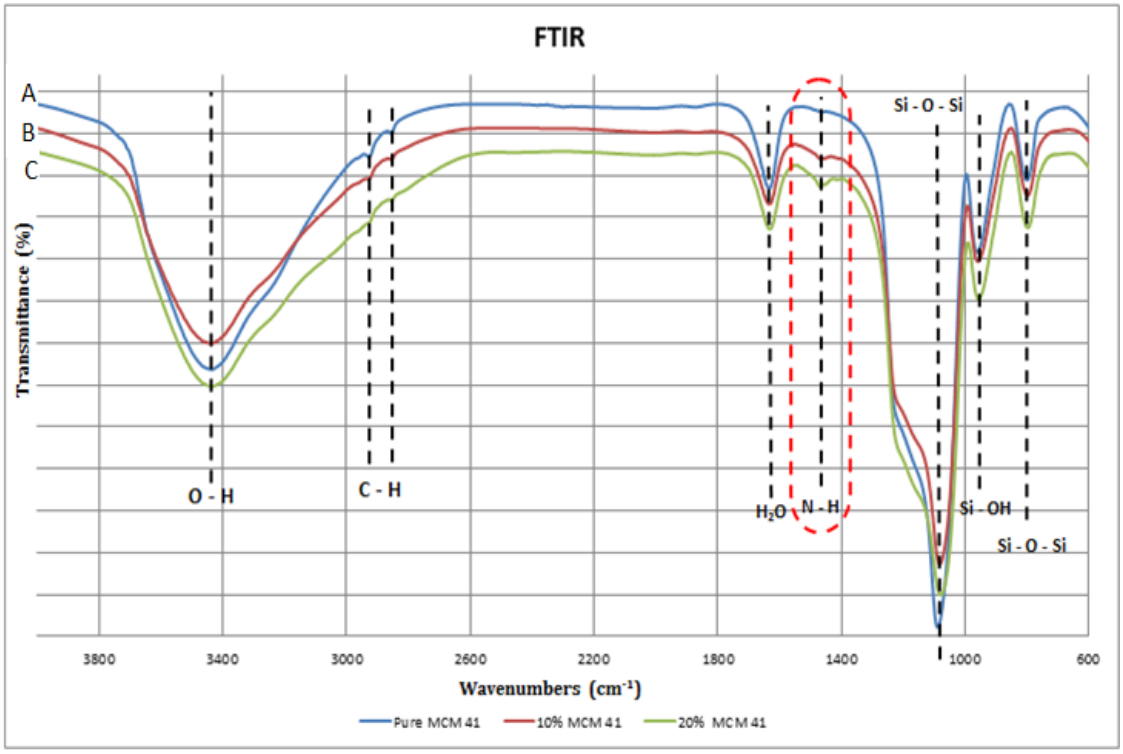

Figure 5:FTIR spectra of (A) pure Mesoporous Silica MCM 41 and modified Mesoporous Silica MCM 41, (B) 10% additional AEPTMS and (C) 20% additional AEPTMS.

Figure 5 shows the FTIR spectra of (A) pure Mesoporous Silica MCM 41 and modified Mesoporous Silica MCM 41, with 10% additional AEPTMS (B) and 20% additional AEPTMS(C). Peak at 980 $cm^{-1}$is observed for all spectra which represent the symmetric vibration of typical Si-O-Si. The strong peaks at 1110 cm^{-1} are attributed to the stretching frequencies for asymmetric stretching vibration of typical

Si-O-Si (Yuan et al., 2013). These results confirmed that all samples synthesized in the present work show mesoporous silica structure. Referring to Figure 5, the absorbance peaks around 800 cm^{-1}in all the samples is attributed to the presence of Si-OH. The absorption peaks at 2840 cm^{-1} and 2950 cm^{-1} for all spectra are assigned to the anchored ethyl group; C-H group in the samples. The absorption peaks at 1620 cm^{-1}, indicates the adsorbed water, H-O-H stretch band. The present of amino groups by N-H can be confirmed at absorption peaks at1490 cm^{-1}. Amino groups started to appear at spectra (B) and (C), with the presence of the stronger N-H peak in spectra (C) as compared to spectra (A) and (B). These results show AEPTMS was successfully incorporated into MCM 41 structure and it can be deduce that the pore surface of MCM 41 has been successfully modified by adding amino groups.

4.1.2 N_2 Adsorption – Desorption Analysis

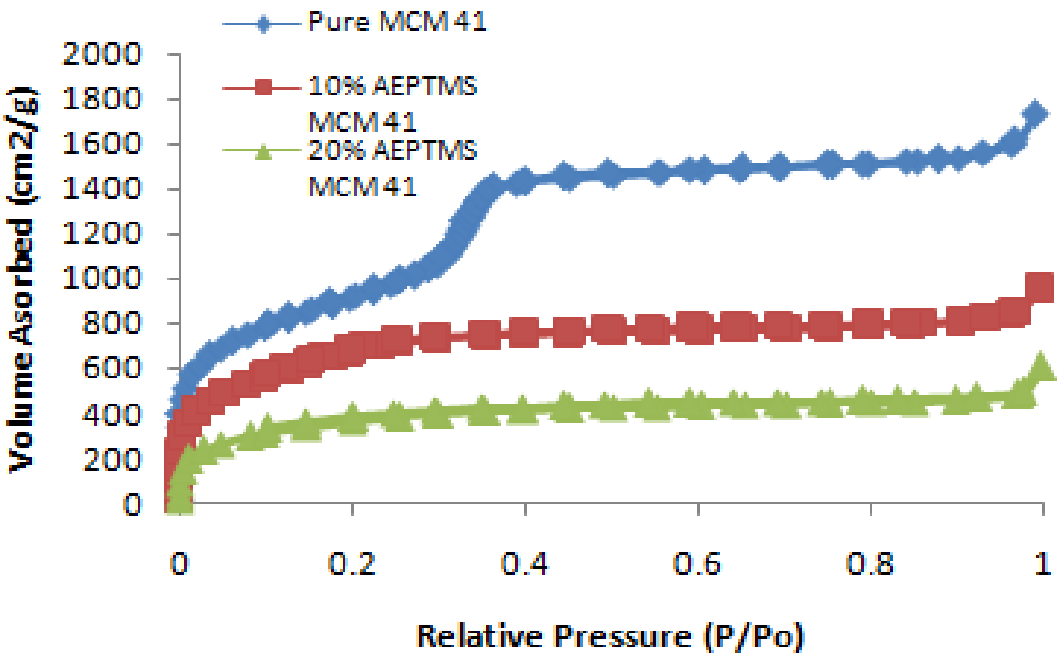

Figure 6: N_2adsorption–desorption isotherms for (A) Pure MCM 41 (B) 10% AEPTMS – MCM 41 and (C) 20% AEPTMS – MCM 41

Figure 6 shows the N_2 adsorption–desorption isotherms for (A) Pure MCM 41 (B) 10% AEPTMS – MCM 41 and (C) 20% AEPTMS – MCM 41. The isotherms

of the samples are approximately similar and in trend with increasing volume adsorbed. Thus, it can be concluded that the shape of the hexagonal arrays of mesopores in MCM-41 was not much affected. For isotherm of pure MCM, it can be observed that two adsorption–desorption hysteresis loops exist. For the first hysteresis loop, in the P/P_0 range around 0.28 to 0.34 caused by the mesopores in Silica layer after template removal. While for the second hysteresis loop, range in P/P_0 more than 0.9 should be representing the mesopores of MCM 41 itself (Villa et al., 2009). As for isotherms of modified MCM, the first hysteresis loop that range in P/P_0 around 0.28 to 0.34 has disappeared, leaving only the second loop, range in P/P_0 more than 0.9. This is because AEPTMS had successfully modified the mesoporous silica layer, thus caused the pore blocking of the mesopores structure.

Table 10: Pore properties of the samples.

Samples	**S_{BET} (m^2/g)**	**V_{total} ($cm^{3/}g$)**	**$d_{average}$ (nm)**	**Reference**
Pure MCM 41	870.29	0.60	2.75	This work
10% AEPTMS – MCM 41	415.69	0.32	3.10	This work
20% AEPTMS – MCM 41	227.97	0.20	3.43	This work
Magnetic-nanocomposemseoporous silica	283.00	0.35	3.80	(Zhao, W.R. et al., 2005)
Fe_3O_4@SiO_2Mesoporous Silica	365.00	0.29	2.30	(Deng, Y.H. etal., 2008)
Hematite-Nanoparticles Mesoporous Silica	445.00	0.29	2.10	(Guo, X.H. et al., 2009)

Table 10 compares the BET surface area, average pore diameter and total pore volume of pure MCM 41 and modified MCM 41 samples. From the tabulated data of the three samples, the values of the pore properties for pure MCM 41 are

higher than that of the values of the pore properties of modified MCM 41. This is caused by the amino group, which is correspondence with the results obtained. As shown in table 10, the surface area, pore diameter and pore volume of 10% AEPTMS – MCM 41are 415.69 m^2/g, 3.10 nm and 0.32 cm^3/g, whereas for 20% AEPTMS – MCM 41, values of 227.97 m^2/g, 3.43 nm and 0.20 cm^3/g are obtained. For modified MCM 41, 10% AEPTMS – MCM 41 exhibited higher surface area and pore volume whereas 20% AEPTMS – MCM 41 demonstrated lower surface area and pore volume compared with other synthesized mesoporous samples reported in the literature based on table 10. It can be concluded that 10% AEPTMS – MCM 41 has larger surface area and pores volume compares to other modified MCM 41 on table 10. These make the adsorbent can absorb enough AEPTMS and contain larger pore size that will increases the loading of amino groups (Yuan, Q. et al., 2013). These results further verify that the AEPTMS are located not only on the outer surfaces but also on the inside of the mesopores.

4.2 Overall Copper Removal of Samples

Table 11: Copper Removal

Samples	**Cu^{2+} removal (%)**	**Reference**
Pure MCM 41	38.3	This work
10% AEPTMS – MCM 41	57.4	This work
20% AEPTMS – MCM 41	52.2	This work
Amino-functionalized Fe_3O_4@SiO_2	30.8	(Wang, J. et al., 20011)
Amine-functionalized mesoporous Fe_3O_4 nanoparticles	49.0	(Xin, X.D. et al., 2012)
Aminopropyl-MCM-41	30.5	(Yang, W.et al., 2013)

Table 11 show the percentage of copper removal from this work and other literatures. Based on table 11, 10% AEPTMS – MCM 41 show the highest percentage removal; 57.4% compare with other adsorbent, followed by 20%

AEPTMS – MCM 41;52.2%. For pure MCM 41, the percentage of carbon removal was only at 38.3 %. From this table, amino groups have high effect on removal of copper ion compare to other adsorbent.

4.3 Adsorption Isotherms Study

Adsorption isotherm is essential in determining the adsorption performance for an adsorbent. For adsorption isotherms, the adsorbent was used to calculate its adsorption capacity on copper ions.

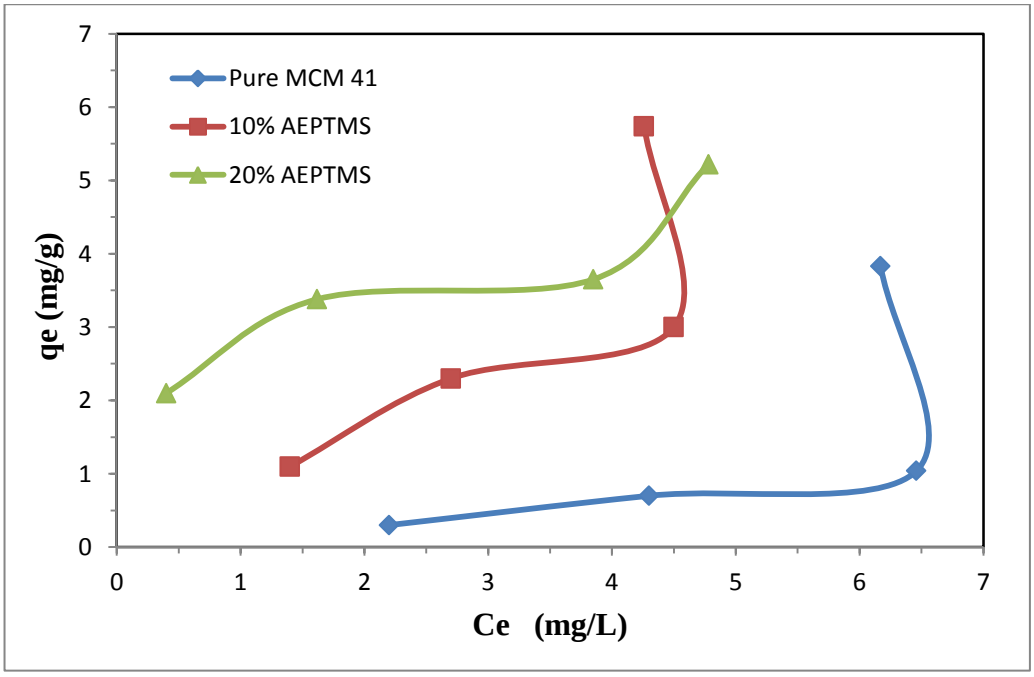

Figure 7: Adsorption Isotherms for different type of MCM 41 on copper ions

Figure 7 shows the adsorption isotherm for pure MCM 41, 10% AEPTMS – MCM 41 and 20% AEPTMS – MCM 41 on copper ions. This figure shows that adsorption capacity at equilibrium, q_e increased with increasing in equilibrium concentration, C_e. Based on Figure 7, the modified MCM-41demonstrated higher adsorption capacity compared to pure MCM 41. The higher the amino groups added in the modified MCM 41, the higher the adsorption of copper ion for the materials. When the equilibrium concentration is more than 4 mg/L, 10% AEPTMS – MCM 41 shows the highest adsorption capacity compare with pure MCM 41 and 20% AEPTMS – MCM 41. This is probably due to increase in surface area, pore volume

and pore size of 10% AEPTMS – MCM 41 that improve the adsorption capacity of copper ions.

The adsorption isotherms can be explained by using Langmuir models and Freundlich models. Langmuir model was expressed in Eq(2), whereas Freundlich model-was expressed in Eq(3).

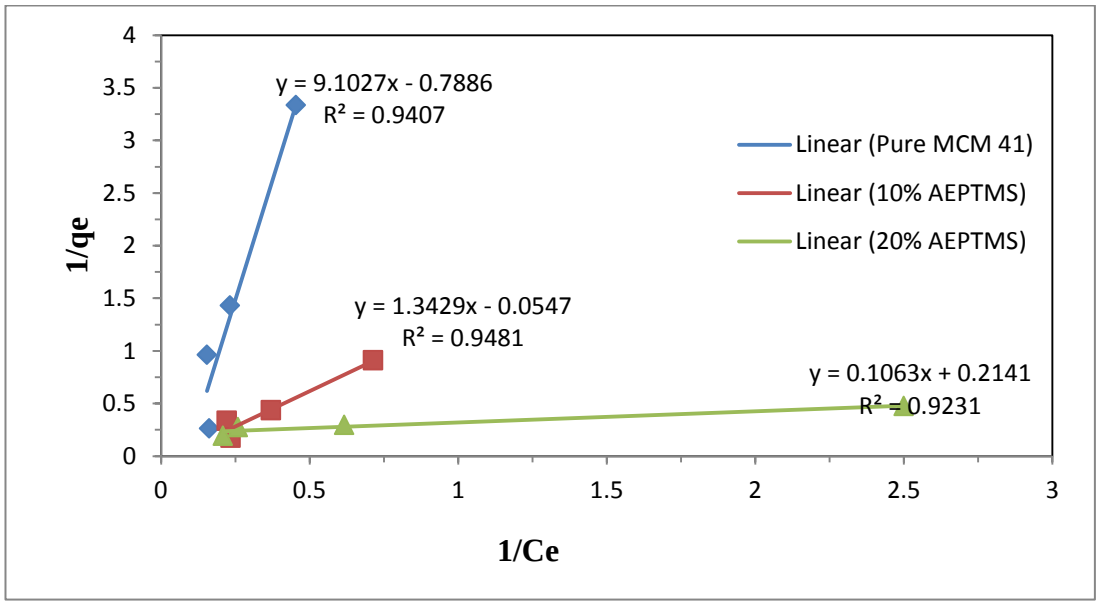

Figure 8: Langmuir plots of copper adsorption on pure MCM 41, 10% AEPTMS – MCM 41 and 20% AEPTMS – MCM 41

The Langmuir model can predict the amount of adsorption occur at specific homogeneous site in the adsorbent along with monolayer sorption (Yuan, Q. et al., 2013). Figure 8 shows the Langmuir plots for all the adsorbents used for copper adsorption in the present work. Referring to Figure 8, Langmuir isotherm equation was used to form straight line by plotting $1/q_e$ versus $1/C_e$. From this plot, the K_L and a_L values were calculated from the slopes $1/K_L$ and intercepts a_L/ K_L. The parameters were tabulate in Table 12. The isotherm data for all sample show high linearity, around $R^2 = 0.92$ until $R^2 = 0.95$. The Langmuir parameters value of K_L and a_L of modified MCM 41, with additional of AEPTMS is higher compared to pure MCM 41. The Langmuir parameters for pure MCM 41, 10% AEPTMS – MCM 41 and 20% AEPTMS – MCM 41 is K_L (L/g) = 0.10987, 0.7452, 9.433 and a_L(L/mg) = -

0.0866, - 0.04002, 2.019. In general, the modified MCM 41 shows higher Langmuir parameters compare to pure MCM 41.

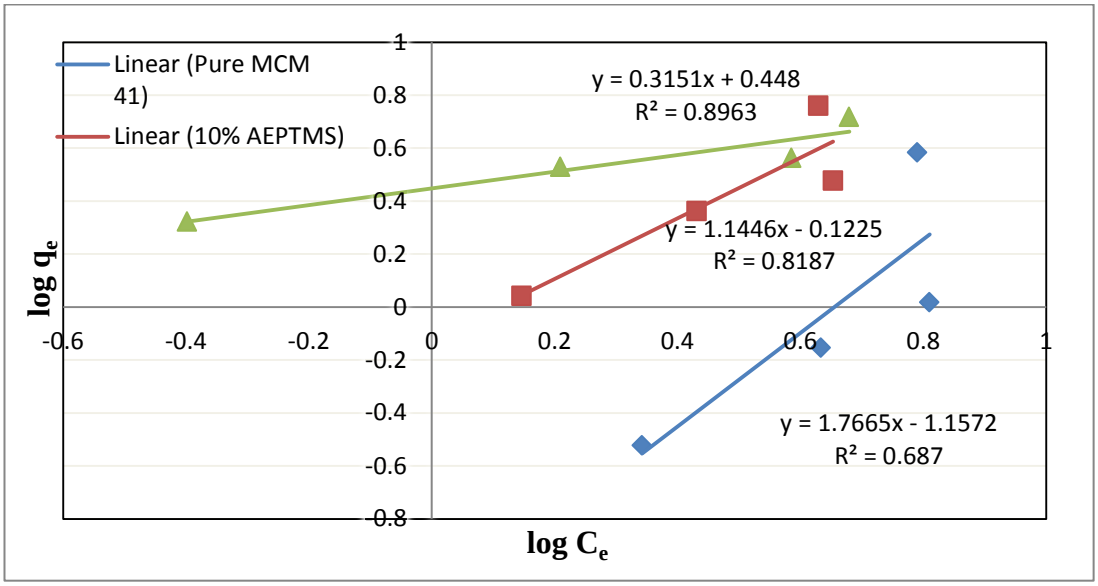

Figure 9: Freundlich plots ofcopper adsorption on pure MCM 41, 10% AEPTMS – MCM 41 and 20% AEPTMS – MCM 41

The Freundlich model can be applied to non ideal adsorption on heterogeneous surfaces and multi layer adsorption (Yuan, Q. et al., 2013). Figure 9, shows the Freundlich plots for the adsorbents on copper adsorption. The straight lines were formed by plotting log q_e versus C_e. For *n* value equalor more than 1indicate as a normal Freundlich isotherm whereas for *n* value lower or less than 1, it can be indicated as cooperative adsorption (Vimonses et al, 2009).Table 12 shows the parameters comparison between two different adsorption isotherm models. Referring to Table 12, the *n* values for pure MCM 41 and 10% AEPTMS – MCM 41 are below 1, thus indicating cooperative adsorption whereas for 20% AEPTMS – MCM 41, it indicates normal Freundlich adsorption. From the Figure9, the Freundlich plots shows positive slope due to positive correlation of the parameters of Freundlich isotherm (log q_e and log C_e). Other than that, the Freundlich plots did not show linearity. The correlation coefficient for pure MCM 41, 10% AEPTMS – MCM 41, 20% AEPTMS – MCM 41 was R^2 = 0.687, 0.818, 0.896.Based on the correlation coefficient value, R^2, it can be concluded that Langmuir model fits better compared to Freundlich model for copper adsorption. These results proved that the adsorption

of copper ion into modified MCM 41 by amino group is generally can be considered as monolayer adsorption process (Seliem, K. et al., 2013).

Table 12: Adsorption isotherm parameters for Pure MCM 41, 10% AEPTMS – MCM 41, 20% AEPTMS – MCM 41 on copper adsorption.

Sample	Langmuir Isotherm			Freundlich Isotherm		
	K_L (L/g)	a_L(L/mmol)	R^2	K_f (L/g)	n	R^2
Pure	0.10987	-0.0866	0.94	0.0696	0.56625	0.687
10%	0.7452	-0.0402	0.948	0.7551	0.87413	0.818
20%	9.433	2.019	0.923	2.8054	3.17460	0.896

4.4 Adsorption Kinetics Study

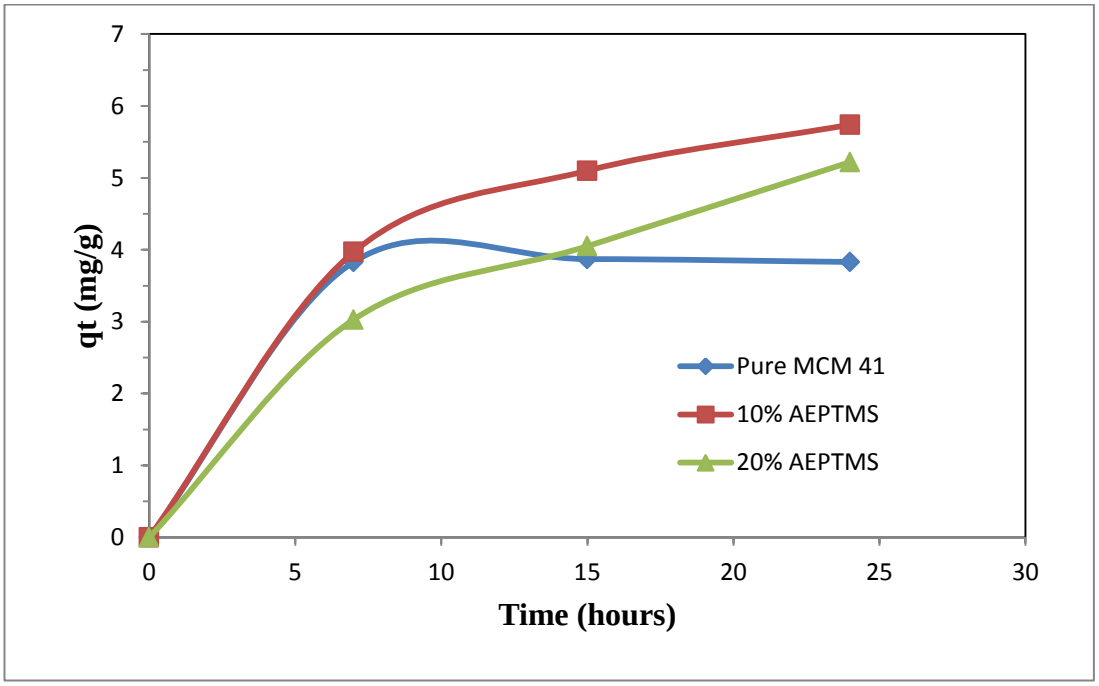

Figure 10: Adsorption kinetic of copper ions on pure MCM 41, 10% AEPTMS – MCM 41 and 20% AEPTMS – MCM 41.

Figure 10 shows the adsorption kinetic of copper ion on pure MCM 41, 10% AEPTMS – MCM 41 and 20% AEPTMS – MCM 41 at room temperature. From the figure, the kinetic behavior of the sample can be divided into two stages; first stage is rapid adsorption that occurs for the first 7 hours and continues for the second stage

that is slower adsorption, which is much lower compare to the initial stage. Besides, pure MCM 41 reached adsorption equilibrium more faster compare to modified MCM 41. The first stage adsorption demonstrated high adsorption kinetic behavior due to higher number of vacant mesopores available in the samples to adsorb copper ions. For the second stage adsorption, the process is slowing down due to the decrease in the number of vacant mesopores, thus create lower changes for the adsorption of copper ions to occur. Pure MCM 41 requires 7 hours to reach adsorption equilibrium, whereas for 10% AEPTMS – MCM 41 and 20% AEPTMS – MCM 41, more than24 hours is required for the process to reach equilibrium. Referring to Figure 10, modified MCM-41 samples show higher adsorption capability as compared to pure MCM-41 sample , while 10% AEPTMS – MCM 41 exhibits higher adsorption ability compared20% AEPTMS – MCM 41. It can be concluded that 10% AEPTMS – MCM 41 has the optimum mesopores – amino sites that available for adsorption of copper ions.

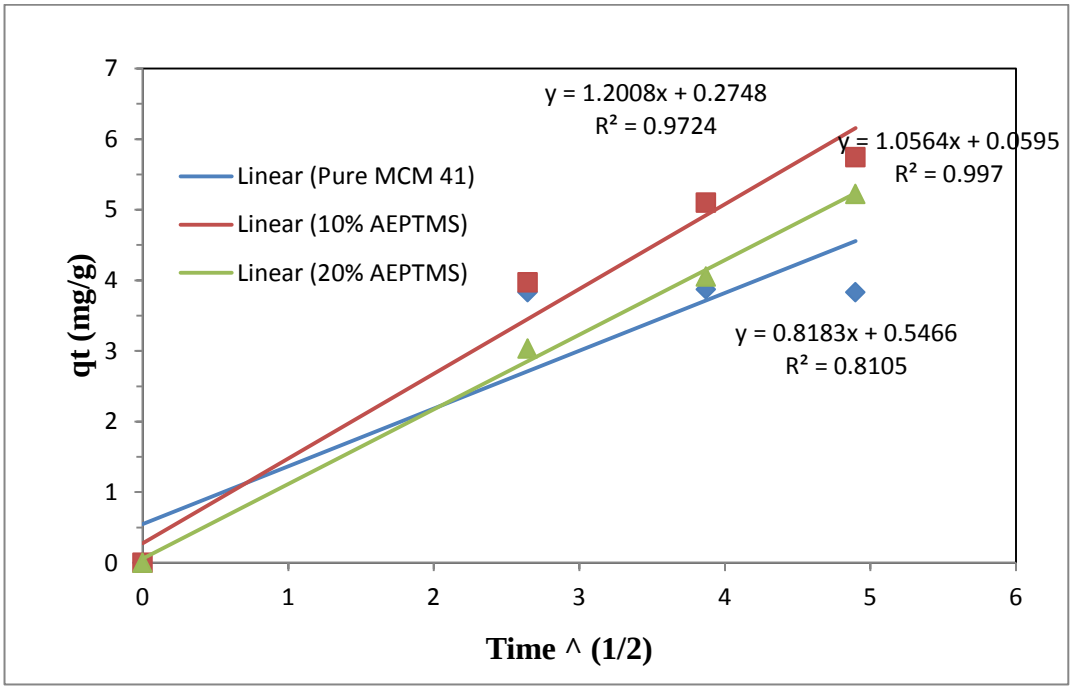

Figure 11: Weber and Morris intra particle diffusion for pure MCM 41, 10% AEPTMS – MCM 41 and 20% AEPTMS – MCM 41.

Table 13: Weber and Morris intra particle diffusion for pure MCM 41, 10% AEPTMS – MCM 41 and 20% AEPTMS – MCM 41

Adsorbent	**Intra Particle Diffusion Model**		
	K_p (mg / g hour)	**C (mg/g)**	**R^2**
Pure MCM 41	0.818	0.546	0.81
10% AEPTMS - MCM 41	1.2	0.274	0.972
20% AEPTMS - MCM 41	1.056	0.059	0.997

Figure 11 shows the Weber and Morris intra particle diffusion of pure MCM 41, 10% AEPTMS – MCM 41 and 20% AEPTMS – MCM 41. For more details, intra - particle diffusion/transport process were calculated from the adsorption kinetic data by using Weber and Morris equation (Demiral et al., 2010):

$$q_t = k_p t^{1/2} + C \quad (7)$$

where k_p is the rate constant of the intra particle diffusion and C is the film thickness. All the data calculated and corresponding coefficient were given in Table 13. For this model, if the plot is straight line and passes throughout the origin, it indicates that this process is controlled by intra particle diffusion only. If variation exists, it shows that more than two steps affect the adsorption process (Demiral et al., 2010). From figure 11, the intercept (C value) of pure MCM 41, 10% AEPTMS – MCM 41, 20% AEPTMS – MCM 41 is 0.546, 0.274 and 0.059, respectively. This shows that the plot is linear but does not pass throughout the origin, thus it indicates that the adsorption requires a two-step process and not only depends on intra particle diffusion.

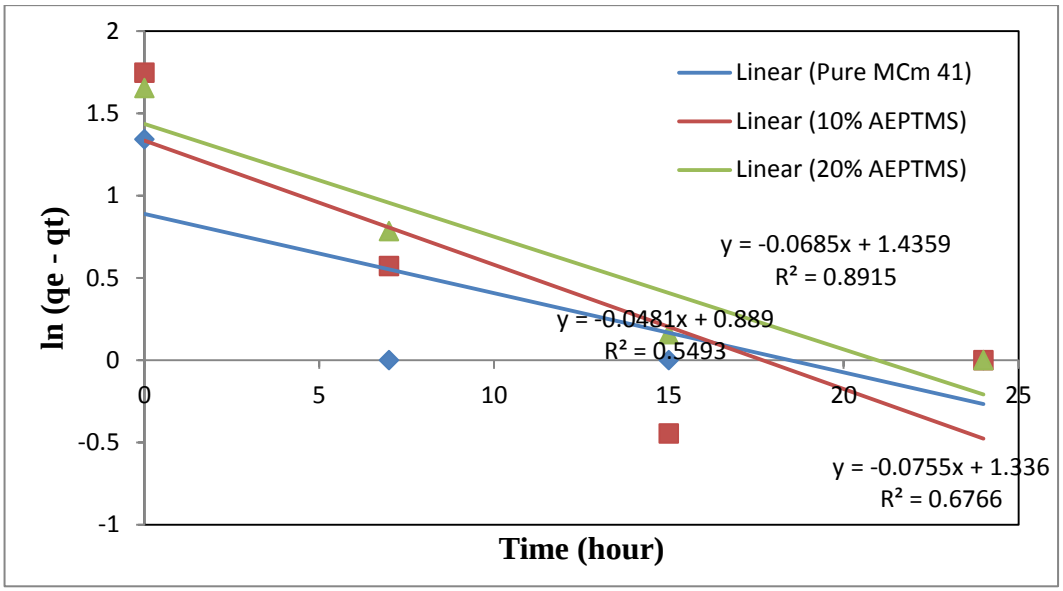

Figure 12: Pseudo-first-order model for copper ions adsorption by pure MCM 41, 10% AEPTMS – MCM 41 and 20% AEPTMS – MCM 41.

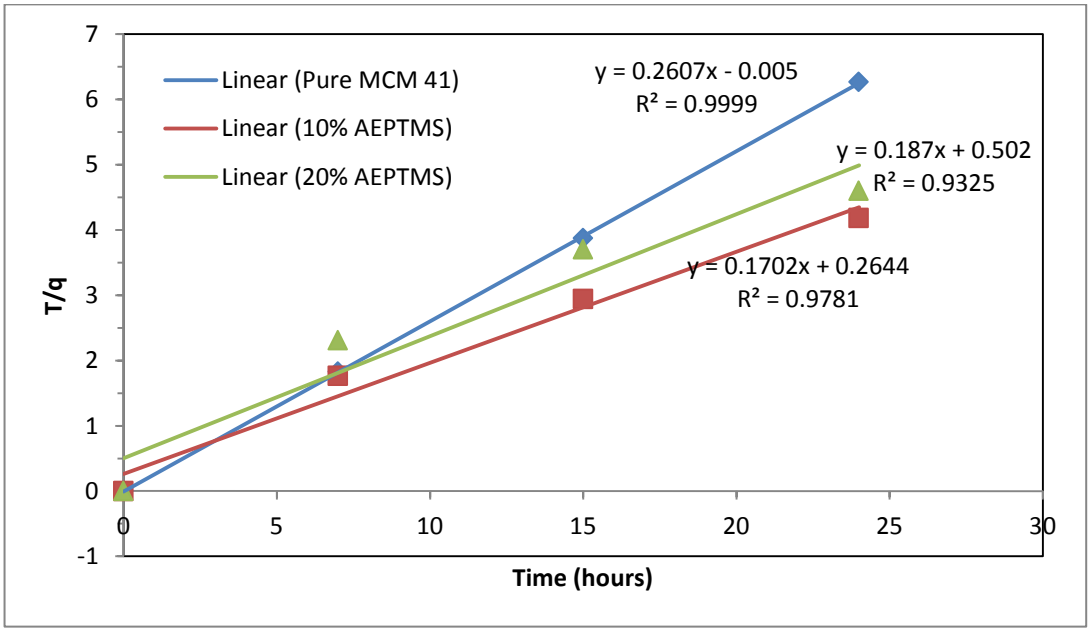

Figure 13: Pseudo-second-order model for copper ions adsorption by pure MCM 41, 10% AEPTMS – MCM 41 and 20% AEPTMS – MCM 41.

Table 14: Pseudo-first-order model and pseudo-second-order model parameters for copper ions adsorption by pure MCM 41, 10% AEPTMS –MCM 41 and 20% AEPTMS – MCM 41

Adsorbent	Pseudo-First-Order Model			Pseudo-Second-Order Model		
	K_1 (1 / hour)	q_{e1} (mg/g)	R^2	K_2 (1 / hour)	Q_{e2} (mg/g)	R^2
Pure MCM 41	0.068	2.433	0.549	6.1014	3.86	0.999
10% AEPTMS - MCM 41	0.075	3.804	0.676	0.1095	5.88	0.978
20% AEPTMS - MCM 41	0.068	4.2	0.891	0.0695	5.35	0.932

The data was further analyzed with its kinetic behavior using pseudo-first-order (Eq. 5) and pseudo-second-order equations (Eq. 6). Figures 12 and 13 show the pseudo-first-order and pseudo-second-order model fitting for copper ions adsorption by MCM 41, 10% AEPTMS – MCM 41 and 20% AEPTMS – MCM 41. The parameters involve in pseudo-first-order and pseudo-second-order are tabulated in table 14. From table 14, the correlation coefficient, R^2 of pseudo-second-order model is more closed to 1 compared with R^2 obtained from pseudo-first-order model. Thus, the adsorption process can be presented by pseudo-second-order model. To summarizes, based on pseudo-second-order model, the copper ions adsorption onto pure MCM 41, 10% AEPTMS – MCM 41 and 20% AEPTMS – MCM 41 possibly will occur by a reaction related to valences forces by sharing or exchange of electrons (Ho et al., 2003).

CHAPTER 5
CONCLUSION AND RECOMENDATION

The present project focuses on the development of functionalized mesoporous silica MCM-41 adsorbents by tertiary amine-functional group, 3-[2-(2-aminoethylamino) ethylamino] propyltrimethoxysilane, AEPTMS. These adsorbents have been synthesized using co-condensation method and characterized using different analytical tools. The resultant adsorbents were tested for its efficiency in Cu^{2+} removal.

In summary, modified amino group mesoporous silica adsorbent was successfully synthesized. Form FTIR, the present of NH group shows that the AEPTMS was successfully incorporated into MCM 41 structure and the pore surface of MCM 41 has been successfully modified by additional of amino groups. The modified mesoporous silica has higher BET surface compare with pure MCM 41.Other than that, the adsorption process on modified MCM 41 can be described by Langmuir Model, which was generally considered as monolayer adsorption process. Furthermore, the adsorption process closely related to pseudo-second-order model, which possibly can occur by a chemical reaction of valences forces by sharing or exchange of electrons.

For copper removal study, the percentage of removal results for copper ions on pure MCM 41, 10% AEPTMS – MCM 41 and 20% AEPTMS – MCM 41 was 38.3%, 57.4% and 52.2%. 10% AEPTMS – MCM 41 have the highest percentage removal of copper ions. Based on the present work, 10% AEPTMS – MCM 41 have the optimum amount of amino group needed for modification and give more positive results for copper adsorption compare with pure MCM 41 and 20% AEPTMS – MCM 41. Therefore, 10% AEPTMS – MCM 41 was an excellent adsorbent for copper ions removal.

For future recommendation, the adsorbent need to be test further with other metal ion so that varies data and measurement can be taken into account. The successful development of functionalized mesoporous silica MCM-41adsorbent by tertiary amine functional group can beneficial to environment especially in reducing heavy metal pollutants.

REFERENCES

Ahalya, N., Ramachandra, T., & Kanamadi, R. (2003). Biosorption of heavy metals. *Res. J. Chem. Environ, 7*(4), 71-79.

Argun, M. E., & Dursun, S. (2006). Removal of heavy metal ions using chemically modified adsorbents. *J. Int. Environ. Appl. Sci, 1*, 27-40.

Bakalár, T., Búgel, M., & Gajdošová, L. (2009). Heavy metal removal using reverse osmosis. *Acta Montanistica Slovaca, 14*(3), 250.

Calvo, A., Joselevich, M., Soler-Illia, G. J. A. A., & Williams, F. J. (2009). Chemical reactivity of amino-functionalized mesoporous silica thin films obtained by co-condensation and post-grafting routes. *Microporous and Mesoporous Materials, 121*(1–3), 67-72. doi: http://dx.doi.org/10.1016/j.micromeso.2009.01.005

Fu, F., & Wang, Q. (2011). Removal of heavy metal ions from wastewaters: a review. *J Environ Manage, 92*(3), 407-418. doi: 10.1016/j.jenvman.2010.11.011

Ge, F., Li, M. M., Ye, H., & Zhao, B. X. (2012). Effective removal of heavy metal ions Cd2+, Zn2+, Pb2+, Cu2+ from aqueous solution by polymer-modified magnetic nanoparticles. *J Hazard Mater, 211-212*, 366-372. doi: 10.1016/j.jhazmat.2011.12.013

Heidari, A., Younesi, H., & Mehraban, Z. (2009). Removal of Ni(II), Cd(II), and Pb(II) from a ternary aqueous solution by amino functionalized mesoporous and nano mesoporous silica. *Chemical Engineering Journal, 153*(1–3), 70-79. doi: http://dx.doi.org/10.1016/j.cej.2009.06.016

Huang, C., Tang, Z., Zhou, Y., Zhou, X., Jin, Y., Li, D., . . . Zhou, S. (2012). Magnetic micelles as a potential platform for dual targeted drug delivery in cancer therapy. *Int J Pharm, 429*(1-2), 113-122. doi: 10.1016/j.ijpharm.2012.03.001

Huh., S., Wienc., J. W., Yoo., J.-C., Prusk., M., & Lin., V. S. Y. (2003). Organic Functionalization and Morphology Control of Mesoporous Silicas via Co-Condensation Synthesis Method. *Chemical Mater, 15*, 4247-4256. doi: 10.1021/cm0210041

Idris, S. A., Davidson, C. M., McManamon, C., Morris, M. A., Anderson, P., & Gibson, L. T. (2011). Large pore diameter MCM-41 and its application for lead removal from aqueous media. *J Hazard Mater, 185*(2–3), 898-904. doi: http://dx.doi.org/10.1016/j.jhazmat.2010.09.105

Ji, F., Li, C., Tang, B., Xu, J., Lu, G., & Liu, P. (2012). Preparation of cellulose acetate/zeolite composite fiber and its adsorption behavior for heavy metal ions in aqueous solution. *Chemical Engineering Journal, 209*, 325-333. doi: 10.1016/j.cej.2012.08.014

Juang, R.-S., Xu, Y.-Y., & Chen, C.-L. (2003). Separation and removal of metal ions from dilute solutions using micellar-enhanced ultrafiltration. *Journal of Membrane Science, 218*(1-2), 257-267. doi: 10.1016/s0376-7388(03)00183-2

Lee, H. W., Cho, H. J., Yim, J.-H., Kim, J. M., Jeon, J.-K., Sohn, J. M., . . . Park, Y.-K. (2011). Removal of Cu(II)-ion over amine-functionalized mesoporous silica materials. *Journal of Industrial and Engineering Chemistry, 17*(3), 504-509. doi: http://dx.doi.org/10.1016/j.jiec.2010.09.022

Lo, S.-F., Wang, S.-Y., Tsai, M.-J., & Lin, L.-D. (2012). Adsorption capacity and removal efficiency of heavy metal ions by Moso and Ma bamboo activated carbons. *Chemical Engineering Research and Design, 90*(9), 1397-1406. doi: 10.1016/j.cherd.2011.11.020

Mashhadizadeh, M. H., Amoli-Diva, M., Shapouri, M. R., & Afruzi, H. (2014). Solid phase extraction of trace amounts of silver, cadmium, copper, mercury, and lead in

various food samples based on ethylene glycol bis-mercaptoacetate modified 3-(trimethoxysilyl)-1-propanethiol coated Fe3O4 nanoparticles. *Food Chem, 151*, 300-305. doi: 10.1016/j.foodchem.2013.11.082

Nagata, H., Takimura, M., Yamasaki, Y., & Nakahira, A. (2006). Syntheses and Characterization of Bulky Mesoporous Silica MCM-41 by Hydrothermal Hot-Pressing Method. *Materials Transactions, 47*(8), 2103-2105. doi: 10.2320/matertrans.47.2103

Nandiyanto, A. B. D., Kim, S.-G., Iskandar, F., & Okuyama, K. (2009). Synthesis of spherical mesoporous silica nanoparticles with nanometer-size controllable pores and outer diameters. *Microporous and Mesoporous Materials, 120*(3), 447-453. doi: http://dx.doi.org/10.1016/j.micromeso.2008.12.019

Pérez-Quintanilla, D., Sánchez, A., del Hierro, I., Fajardo, M., & Sierra, I. (2007). Preparation, characterization, and Zn2+ adsorption behavior of chemically modified MCM-41 with 5-mercapto-1-methyltetrazole. *Journal of Colloid and Interface Science, 313*(2), 551-562. doi: http://dx.doi.org/10.1016/j.jcis.2007.04.063

Singanan, M., & Peters, E. (2013). Removal of toxic heavy metals from synthetic wastewater using a novel biocarbon technology. *Journal of Environmental Chemical Engineering, 1*(4), 884-890. doi: 10.1016/j.jece.2013.07.030

Singh, R., Gautam, N., Mishra, A., & Gupta, R. (2011). Heavy metals and living systems: An overview. *Indian journal of pharmacology, 43*(3), 246.

Taib, N. I., Endud, S., & Katun, M. N. (2011). Functionalization of Mesoporous Si-MCM-41 by Grafting with Trimethylchlorosilane. *International Journal of Chemistry, 3*(3). doi: 10.5539/ijc.v3n3p2

Teraoka, Y., Ishida, S., Yamasaki, A., Tomonaga, N., Yasutake, A., Izumi, J., . . . Kagawa, S. (2001). Synthesis and characterization of tin oxide-modified mesoporous silica by the repeated post-grafting of tin chloride. *Microporous and Mesoporous Materials, 48*(1–3), 151-158. doi: http://dx.doi.org/10.1016/S1387-1811(01)00338-9

Wang, S. Y., Tsai, M. H., Lo, S. F., & Tsai, M. J. (2008). Effects of manufacturing conditions on the adsorption capacity of heavy metal ions by Makino bamboo charcoal. *Bioresour Technol, 99*(15), 7027-7033. doi: 10.1016/j.biortech.2008.01.014

Yang, J., Tao, H., Ma, H., & Frost, R. (2006). Synthesis of MCM-41 Mesoporous Silica by Microwave Irradiation and ZnO Nanoparticles Confined in MCM-41. *CHINESE JOURNAL OF PROCESS ENGINEERING, 6*, 268.

Yang, W., Ding, P., Zhou, L., Yu, J., Chen, X., & Jiao, F. (2013). Preparation of diamine modified mesoporous silica on multi-walled carbon nanotubes for the adsorption of heavy metals in aqueous solution. *Applied Surface Science, 282*, 38-45. doi: 10.1016/j.apsusc.2013.05.028

Yokoi, T., Kubota, Y., & Tatsumi, T. (2012). Amino-functionalized mesoporous silica as base catalyst and adsorbent. *Applied Catalysis A: General, 421-422*, 14-37. doi: 10.1016/j.apcata.2012.02.004

Yuan, Q., Li, N., Chi, Y., Geng, W., Yan, W., Zhao, Y., . . . Dong, B. (2013). Effect of large pore size of multifunctional mesoporous microsphere on removal of heavy metal ions. *J Hazard Mater, 254-255*, 157-165. doi: 10.1016/j.jhazmat.2013.03.035

Zamani, C., Illa, X., Abdollahzadeh-Ghom, S., Morante, J., & Rodríguez, A. R. (2009). Mesoporous silica: a suitable adsorbent for amines. *Nanoscale research letters, 4*(11), 1303-1308.

Zhou, H., Zhou, X., Zeng, M., Liao, B.-H., Liu, L., Yang, W.-T., . . . Wang, Y.-J. (2014). Effects of combined amendments on heavy metal accumulation in rice (Oryza sativa L.) planted on contaminated paddy soil. *Ecotoxicology and Environmental Safety, 101*(0), 226-232. doi: http://dx.doi.org/10.1016/j.ecoenv.2014.01.001

APPENDIX

Appendix 1 - Synthesis Process

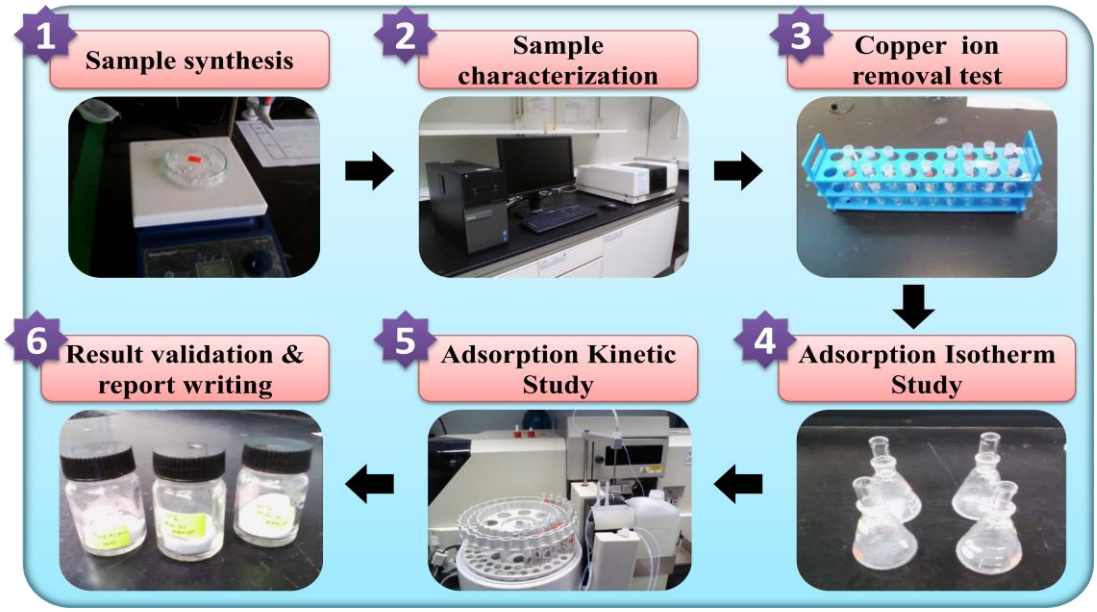

Appendix 2–Characteristics Process

FTIR Equipment:

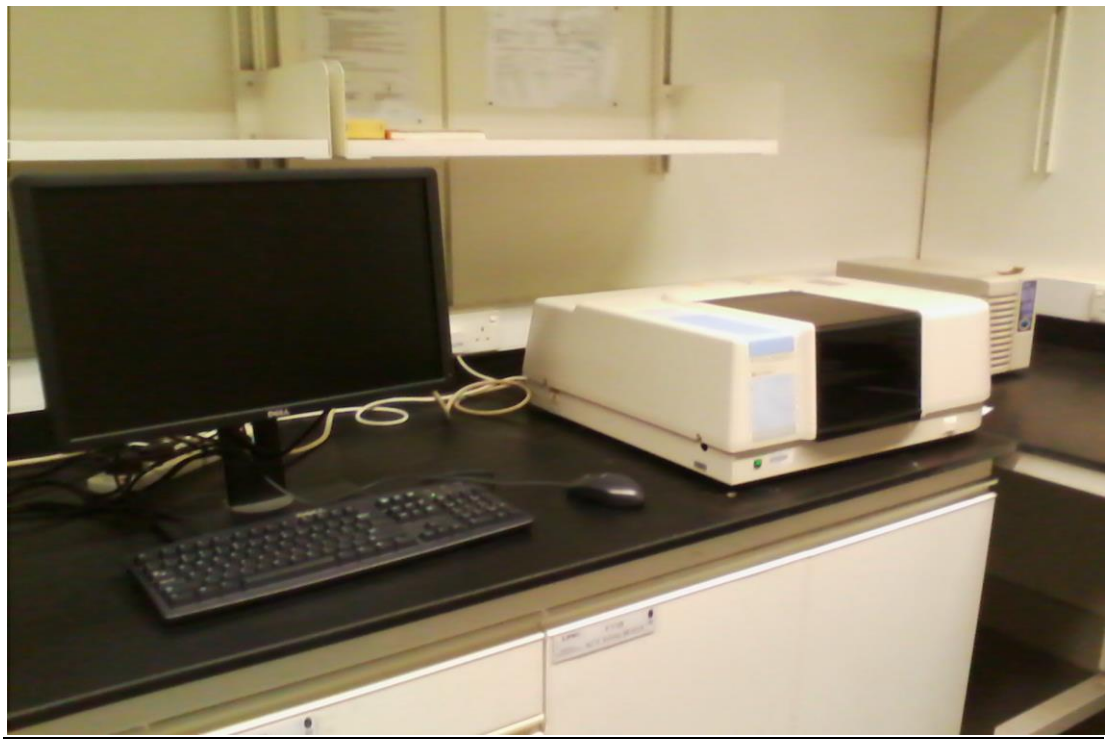

Appendix 3–Removal Process

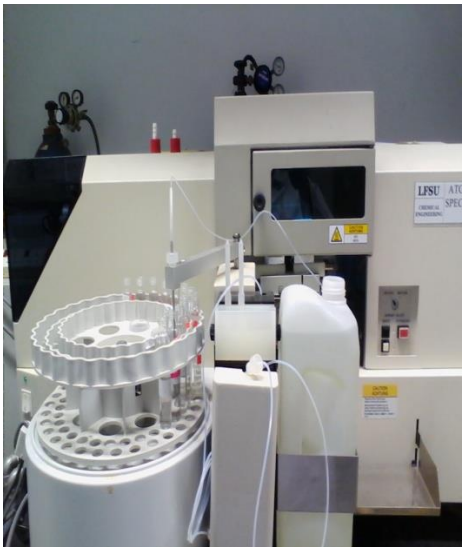

Appendix 4–Kinetics and Isotherms Study

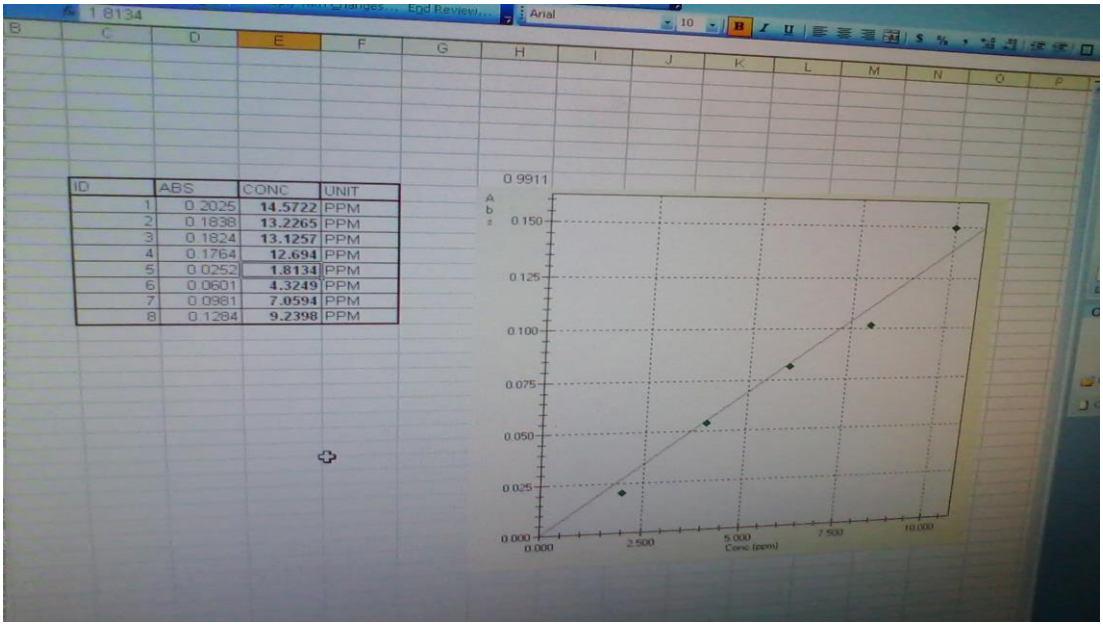

ID	ABS	CONC	UNIT
1	0.2025	**14.5722**	PPM
2	0.1838	**13.2265**	PPM
3	0.1824	**13.1257**	PPM
4	0.1764	**12.694**	PPM
5	0.0252	**1.8134**	PPM
6	0.0601	**4.3249**	PPM
7	0.0981	**7.0594**	PPM
8	0.1284	**9.2398**	PPM

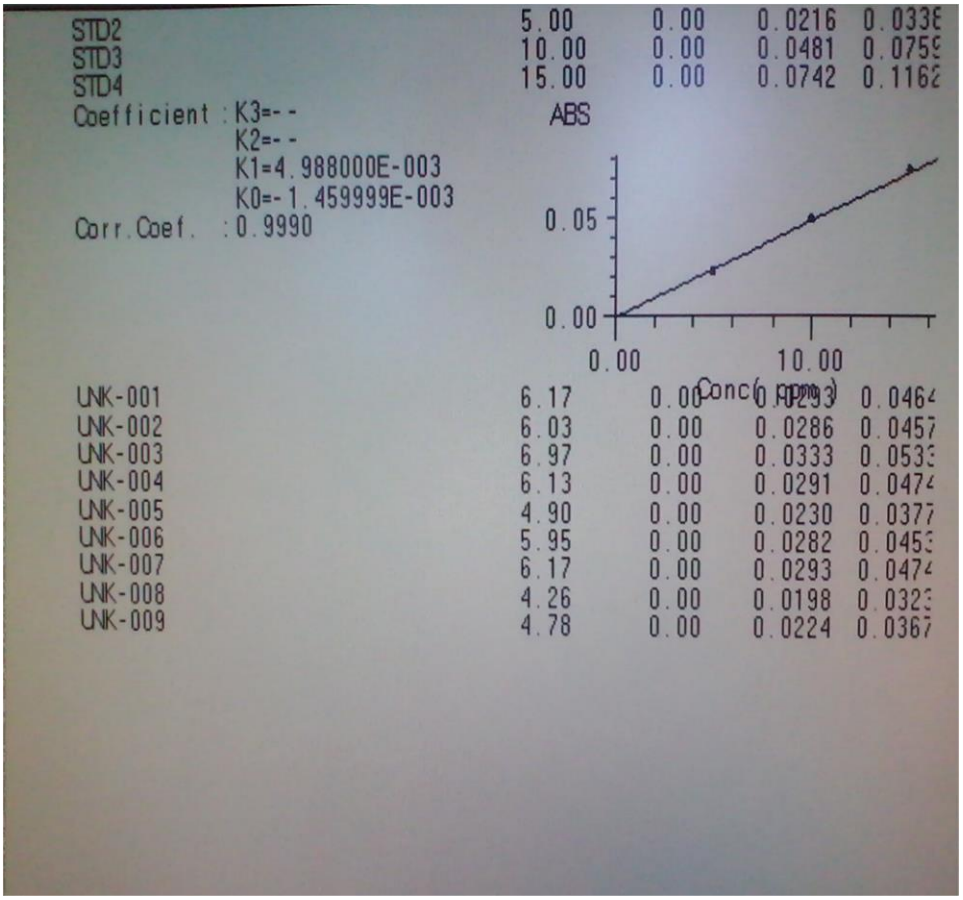

STD2 5.00 0.00 0.0216 0.033E
STD3 10.00 0.00 0.0481 0.075?
STD4 15.00 0.00 0.0742 0.116?

Coefficient : K3=- -
K2=- -
K1=4.988000E-003
K0=-1.459999E-003
Corr.Coef. : 0.9990

ABS
0.05
0.00
0.00
10.00
Conc(ppm)

UNK-001	6.17	0.00	0.0293	0.046?
UNK-002	6.03	0.00	0.0286	0.0457
UNK-003	6.97	0.00	0.0333	0.053?
UNK-004	6.13	0.00	0.0291	0.047?
UNK-005	4.90	0.00	0.0230	0.0377
UNK-006	5.95	0.00	0.0282	0.045?
UNK-007	6.17	0.00	0.0293	0.047?
UNK-008	4.26	0.00	0.0198	0.032?
UNK-009	4.78	0.00	0.0224	0.0367

SYNTHESIS AND CHARACTERIZATION OF FUNCTIONALIZED MESOPOROUS SILICA MCM-41 AS ADSORBENT FOR COPPER IONS REMOVAL

MUHAMMAD HANIF BIN YUSOFF

CHEMICAL ENGINEERING

UNIVERSITI TEKNOLOGI PETRONAS

MAY 2014